NASA/CR–2001–210849

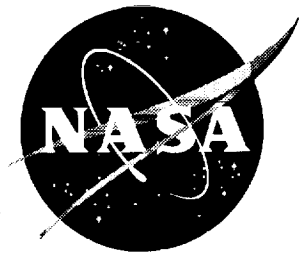

Inviscid Flow Computations of the Orbital Sciences X-34 Over a Mach Number Range of 1.25 to 6.0

Ramadas K. Prabhu
Lockheed Martin Engineering & Sciences Company, Hampton, Virginia

April 2001

The NASA STI Program Office ... in Profile

Since its founding, NASA has been dedicated to the advancement of aeronautics and space science. The NASA Scientific and Technical Information (STI) Program Office plays a key part in helping NASA maintain this important role.

The NASA STI Program Office is operated by Langley Research Center, the lead center for NASA's scientific and technical information. The NASA STI Program Office provides access to the NASA STI Database, the largest collection of aeronautical and space science STI in the world. The Program Office is also NASA's institutional mechanism for disseminating the results of its research and development activities. These results are published by NASA in the NASA STI Report Series, which includes the following report types:

- TECHNICAL PUBLICATION. Reports of completed research or a major significant phase of research that present the results of NASA programs and include extensive data or theoretical analysis. Includes compilations of significant scientific and technical data and information deemed to be of continuing reference value. NASA counterpart of peer-reviewed formal professional papers, but having less stringent limitations on manuscript length and extent of graphic presentations.

- TECHNICAL MEMORANDUM. Scientific and technical findings that are preliminary or of specialized interest, e.g., quick release reports, working papers, and bibliographies that contain minimal annotation. Does not contain extensive analysis.

- CONTRACTOR REPORT. Scientific and technical findings by NASA-sponsored contractors and grantees.

- CONFERENCE PUBLICATION. Collected papers from scientific and technical conferences, symposia, seminars, or other meetings sponsored or cosponsored by NASA.

- SPECIAL PUBLICATION. Scientific, technical, or historical information from NASA programs, projects, and missions, often concerned with subjects having substantial public interest.

- TECHNICAL TRANSLATION. English-language translations of foreign scientific and technical material pertinent to NASA's mission.

Specialized services that help round out the STI Program Office's diverse offerings include creating custom thesauri, building customized databases, organizing and publishing research results... even providing videos.

For more information about the NASA STI Program Office, see the following:

- Access the NASA STI Program Home Page at ***http://www.sti.nasa.gov***

- E-mail your question via the Internet to help@sti.nasa.gov

- Fax your question to the NASA STI Help Desk at (301) 621–0134

- Phone the NASA STI Help Desk at (301) 621–0390

- Write to:
  NASA STI Help Desk
  NASA Center for AeroSpace Information
  7121 Standard Drive
  Hanover, MD 21076–1320

NASA/CR–2001–210849

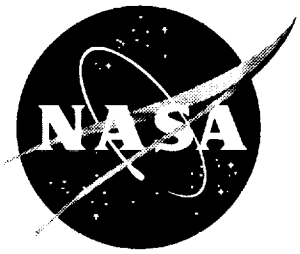

Inviscid Flow Computations of the Orbital Sciences X-34 Over a Mach Number Range of 1.25 to 6.0

Ramadas K. Prabhu
Lockheed Martin Engineering & Sciences Company, Hampton, Virginia

National Aeronautics and
Space Administration

Langley Research Center
Hampton, Virginia 23681–2199

Prepared for Langley Reseach Center
under contract NAS1-96014

April 2001

Available from the following:

NASA Center for AeroSpace Information (CASI)
7121 Standard Drive
Hanover, MD 21076–1320
(301) 621–0390

National Technical Information Service (NTIS)
5285 Port Royal Road
Springfield, VA 22161–2171
(703) 487–4650

Summary

This report documents the results of a computational study conducted to compute the inviscid longitudinal aerodynamic characteristics of the Orbital Sciences X-34 vehicle over a Mach number range of 1.25 to 6.0. The unstructured grid software FELISA was used and the aerodynamic characteristics were computed for Mach numbers of 1.25, 1.6, 2.5, 4.0, 4.63, and 6.0, over an angle of attack range of -4 to 32 degrees. These results were compared with available aerodynamic data from wind tunnel tests on X-34 models. The comparison showed very good agreement in normal force coefficients over the entire Mach number and angle of attack ranges. The computed pitching moment coefficients compared well at Mach numbers 2.5 and above, and at angles of attack of up to 12 deg. The agreement was not good at higher angles of attack possibly due to viscous effects. At lower Mach numbers (1.6 and 1.25) there were significant differences between computed and measured pitching moment coefficient values; this is also attributed to viscous effects. Since the present computations are inviscid, the computed axial force coefficients were consistently lower than the measured values as expected.

Nomenclature

C_A	Axial force coefficient
C_N	Normal force coefficient
C_m	Pitching moment coefficient about the point (0.877, 0, -14.0)
C_p	$(p - p_\infty)/q_\infty$, Pressure coefficient
l_{ref}	Reference length for pitching moment (=5.8167 in.)
M_∞	Freestream Mach number
p_∞	Freestream static pressure
q_∞	$\gamma p_\infty M_\infty^2/2$, Freestream dynamic pressure
S_{ref}	Reference area (=27.2 sq. in.)
x, y, z	Cartesian co-ordinates of a given point; (The origin is at the nose, with the x-axis in the vertical direction, the y-axis in the spanwise direction, and the z-axis in the axial direction pointing into the stream.)
α	Angle of attack, deg.
γ	Ratio of specific heats

Introduction

In a study aimed at providing new space-transportation systems to replace the aging space shuttle, NASA had recommended [1] the development of fully reusable, single-stage-to-orbit concepts. The major requirements for such space transportation systems are low-cost and reliable operations. The X-34 is an industry led program jointly funded by the industry and the Government to develop cheaper and reliable single-stage-to-orbit technology. The X-34 is a Reusable Launch Vehicle (RLV) designed to insert relatively small (1000 - 2000lb.) payloads into earth orbit.

The unmanned rocket powered X-34 RLV would be air launched from a Lockheed L-1011 aircraft at a Mach number of 0.7. After the separation, the liquid rocket motor would fire, and the vehicle would accelerate to sub-orbital speed and reach an altitude of approximately 300,000 ft. At this point the payload

with attached upper stage motor would separate form the RLV. Next, the upper stage motor would fire, sending the payload into the required orbit. After releasing the upper stage, the X-34 reusable vehicle would decelerate, descend, and eventually land on a conventional runway. In this industry/Government partnership venture, Orbital Science Corporation is responsible for designing, building, and flight testing the X-34 vehicle. During the design process, the Aerothermodynamics Branch (AB), NASA Langley Research Center provided much of the wind tunnel testing for the X-34 vehicle to determine the aerodynamic loads and aero-heating at the flight conditions. In addition, AB also provided valuable CFD predictions of the aerodynamic and thermal loads on the X-34 vehicle.

Unstructured grid technology is known to provide quick and reliable CFD solutions to complex flow problems particularly for hypersonic flows. Among the widely used unstructured grid software packages are the FELISA [2] and the TetrUSS [3] systems. In the Aerothermodynamics Branch, FELISA inviscid flow solvers have been used extensively for the prediction of flow over complex vehicles. These flow solvers, like any other inviscid flow solvers, have obvious limitations; because of the absence of a boundary layer there is no skin friction and no flow separation effects. However, the inviscid flow solvers generally yield good normal force and pitching moment results up to a point where the effects of flow separation are not significant.

This paper presents the results of an inviscid computational study for the X-34 vehicle using the unstructured grid software FELISA. A Mach number range of 1.6–6.0 and an angle of attack range of -4–32 is covered in the present study. The results are compared with the experimental data measured in wind tunnel tests conducted on X-34 models in the NASA Langley wind tunnels.

The FELISA Software

All the computations of the present study were done using the unstructured grid software FELISA. This software package has proved to be a powerful tool for fast inviscid flow computations. It consists of a set of computer codes for the generation of unstructured grids of tetrahedral elements and the simulation of three-dimensional steady inviscid flows using these grids. Surface triangulation and discretization of the computational domain using tetrahedral elements are done by two separate codes. There are two flow solvers—one applicable for transonic flows and the other for hypersonic flows with an option for perfect gas air, equilibrium air, and CF_4 gases. Both the solvers were used in the present study. Only the perfect gas option with the specific heat ratio γ=1.4 was used. Post-processors like the aerodynamic analysis routine used in the study, are part of the FELISA software package. More information on FELISA may be found in reference [2].

Geometry

A 1/30th scale wind tunnel model of the X-34 was tested extensively over a Mach number of 0.4–4.63 in the wind tunnels at NASA Langley Research Center. This model has all the major components of the X-34 vehicle, namely, the body, the wing, the rudder, and the bodyflap. However, the engine bell was absent on the model; instead, there was a sting for the model support. This configuration was reproduced in the computational model. A sketch of the X-34 vehicle is shown in Fig. 1. Since the configuration has a plane of symmetry, only one half of the model was simulated in the computational study. The length of the model from its nose to the base is 21.56 inches and the wing semi-span is 5.548 inches. The sting used to mount the model (not shown in the figure) in the wind tunnel test section has a diameter of 1.15 inches. Preliminary computations had indicated that the gaps between the two elevons and the inboard elevon and the body

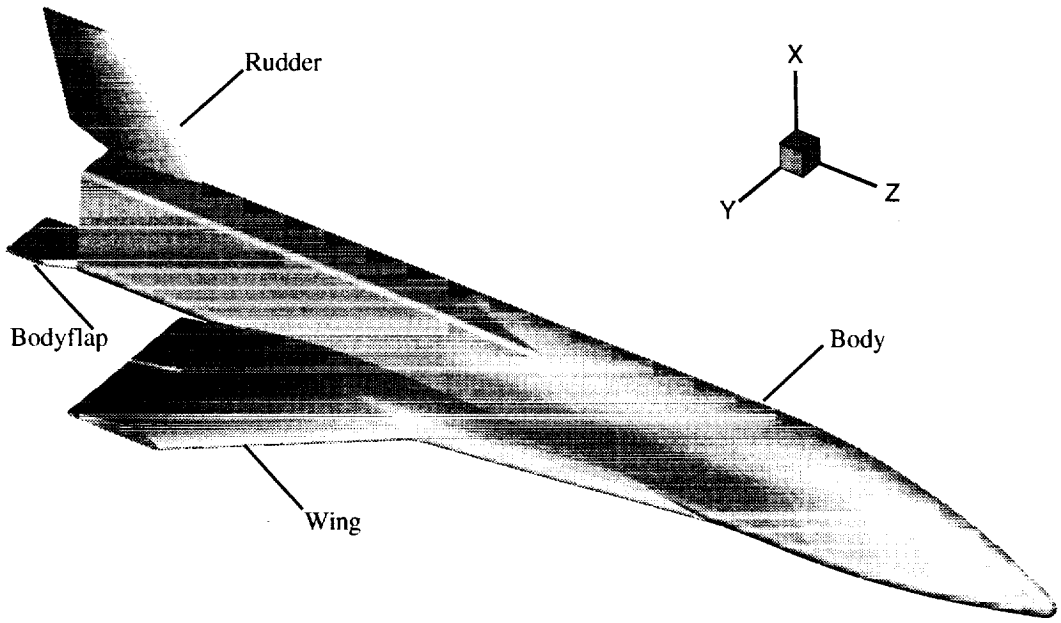

Figure 1: A sketch of the X-34 model.

significantly affected the flow over the upper surface of the elevons. Hence, these gaps were simulated in the computational model. The reference quantities used to normalize the aerodynamic loads are as follows:

Reference area, S_{ref}:	57.2 sq.in.
Reference length for pitching moment, l_{ref}:	5.8167 in.

The pitching moment reference point is at 14.0 inches behind the nose and 0.877 inch above z-axis (the longitudinal axis passing through the nose).

In addition to the 1/30th scale model, two other models of the X-34 were also tested. These are a 1/10-scale model tested (at Mach 0.3) in the NASA Langley 14x22-foot Subsonic Tunnel, and a 0.018 scale model tested in the NASA Langley 20-Inch Mach 6 tunnel.

Computers Used

The surface and volume grid generation, pre-processing of the grids, and post-processing of the solutions were done on an SGI Onyx computer located at the Aerothermodynamics Branch (AB), NASA Langley Research Center. After the necessary FELISA data files were assembled, each surface grid generation required about 30 minutes, and each volume grid generation required 4 to 5 CPU hours on the AB Onyx. The flow solutions were computed on SGI Origin 2000 series parallel computers each having 64 processors and 16G of memory. Each computation of the flow solution required 32 to 40 CPU hours on these parallel machines.

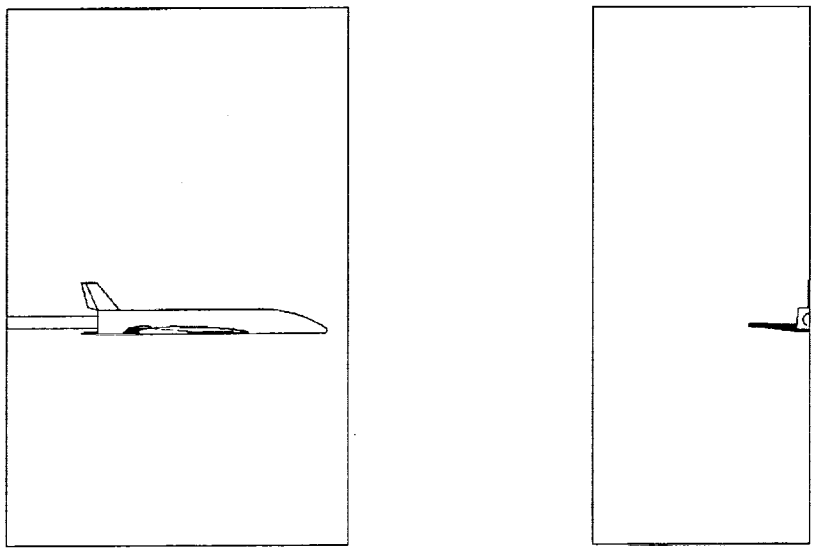

(a) Side view (b) Front view

Figure 2: Computational domain for Mach 1.25 and 1.6.

Grids

The geometrical information of the X-34 model was received in the form of an IGES file. This was processed using the software GridTool [4], and a set of FELISA data files was generated. These data files were used to generate all the grids used in the present study.

Four grids were used in the present study. The computational domains for these grids were chosen to be sufficiently large and away from the body so that except for the exit plane, all the boundary surfaces were in the freestream flow.

A single grid was used for the computations at Mach 1.25 and 1.60. The computational domain used for this grid is shown in Fig. 2. The model surface triangulation for this is shown in Fig. 3. The support sting is present in the CFD model, but is not shown in this figure. The unstructured tetrahedral grid (designated grid 1) for this case has 1,058,983 points. The minimum grid spacing was 0.0043 in. near the nose. The grid spacing near the wing leading edge varied from 0.012 in. at the tip 0.02 in. at the root.

A second grid was built for Mach number 2.5–6.0 computations. The computational domain chosen for this grid is shown in Fig. 4, and the surface triangulation is shown in Figure 5. This grid (designated grid 2) has 1,042,427 points, and a grid spacing of 0.063 in. over the wing upper surface.

Preliminary studies using grid 2 at Mach 2.5 indicated that there were complex flow features over the wing upper surface particularly at angles of attack greater than 8 deg. In order to better resolve these flow features, it was decided to refine the grid over the wing, and a third grid was built. This grid (designated grid 3) has the spacing over the wing reduced to 0.033 in. The spacing in other regions of the grid were unaltered. This grid has 1,262,391 points.

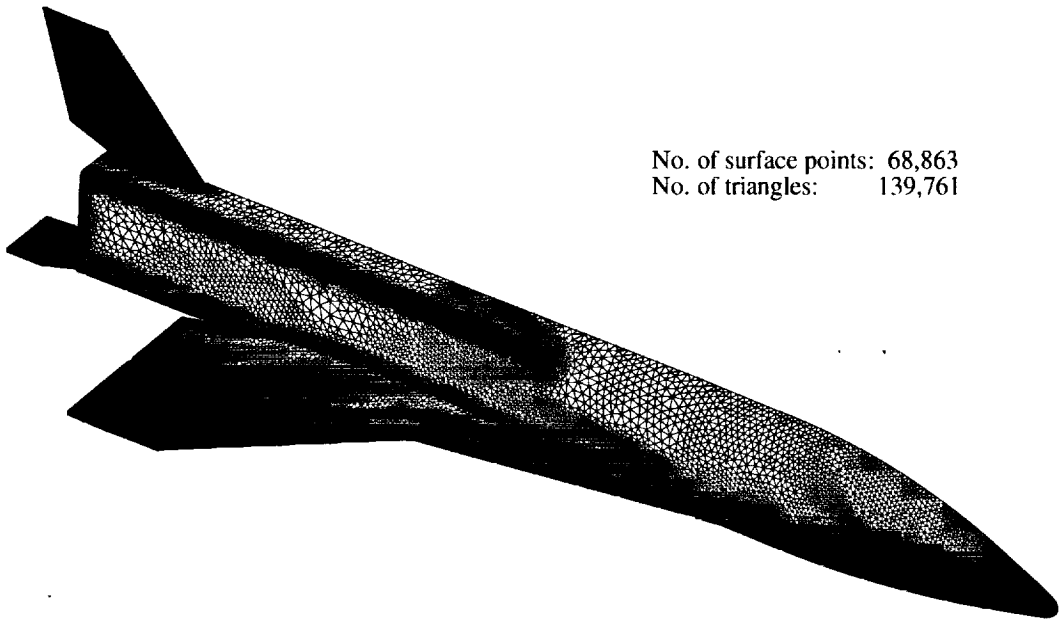

Figure 3: Surface triangulation grid used for Mach 1.25 and 1.6.

The second and the third grids were designed for computations at moderate positive angles of attack. Computations using this grid at -4 deg. angle of attack indicated that this grid may not be suitable for the -4 deg. angle of attack case. Therefore a fourth grid was built for Mach 4.63 computations at -4 deg. angle of attack.

Flow Solution

The grids were partitioned so that the problem could be run on eight processors on a parallel computer. The FELISA transonic as well as the hypersonic flow solvers were used for the flow computations. Each solution was started with the low-order option, and after a few hundred iterations, the higher-order option was turned on, and the solution was run to convergence. After every 50 iteration, the surface pressures were integrated, and the aerodynamic loads, namely the normal and the axial forces, and the pitching moment acting on the model were computed. The flow solution was assumed to be converged when these integrated loads remained essentially constant. Each solution required 32–40 hours of CPU time, i.e., 4–5 wall clock hours. The computed flow solutions were post-processed to obtain the aerodynamic loads. These loads obtained by integrating the surface pressures were non-dimensionalized in the conventional manner, and the aerodynamic coefficients namely, C_N, C_A, and C_m were obtained.

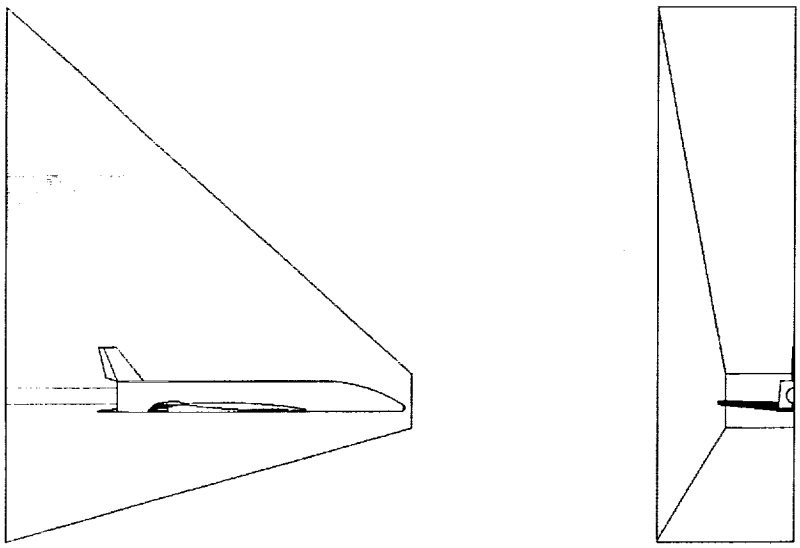

(a) Side view

(b) Front view

Figure 4: Computational domain for Mach 4.63.

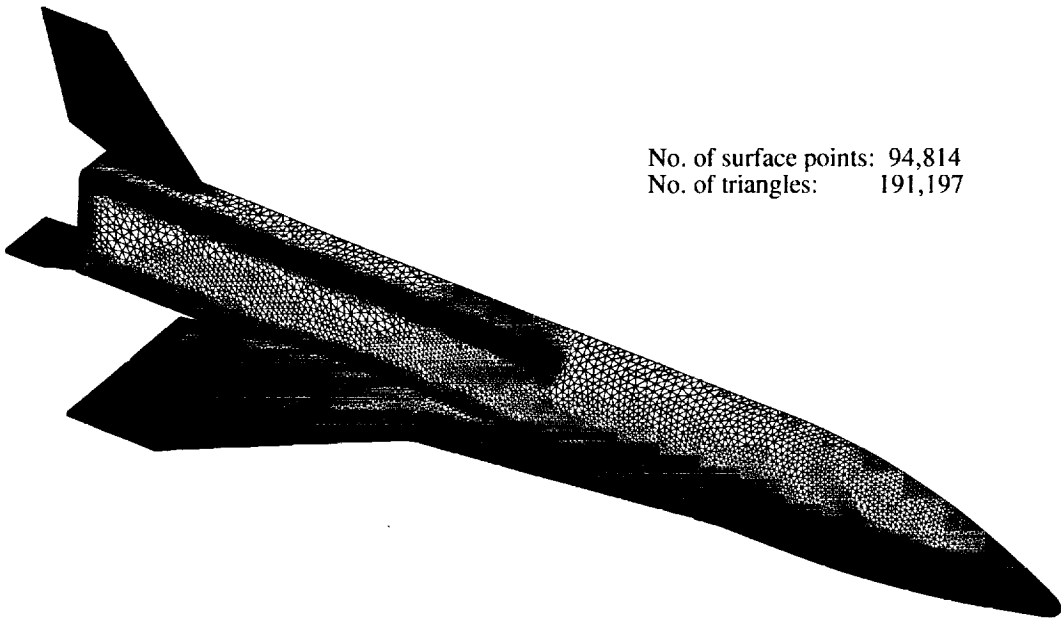

Figure 5: Surface triangulation grid used for Mach 4.63.

Results and Discussion

The computations were done for Mach 1.25, 1.6, 2.5, 4.0, 4.63, and 6.0, over an angle of attack range of -4 to 32 deg. as shown in Table 1. The results of the present computations (C_N, C_A, and C_m) are listed in Tables 2 to 5 and shown plotted in Figures 7 to 13. Available wind tunnel test results are also shown plotted in these figures.

It should be recalled at this point that the present computations are inviscid; hence the boundary layer and skin friction are absent. Absence of the skin friction leads to lower axial forces. The values of C_A are listed in the tables only for the sake of completeness. The computed C_A values would differ from the wind tunnel measured values significantly. Since the boundary layer is absent, the effects of boundary layer separation on the aerodynamic loads are not simulated. At high angles of attack there would be large separated flow regions over the wing upper surface. Further, at transonic speeds in particular, because of the absence of boundary layer in the computations, the shock locations on the computational model would differ from the shock locations on the wind tunnel model. These factors would lead to significant differences in the computed (inviscid) values of aerodynamic coefficients and the wind tunnel measured values.

As noted earlier, three X-34 wind tunnel models were tested extensively in several wind tunnels at NASA Langley Research Center. The tunnels are 14x22-Foot Subsonic Tunnel (1/10-scale model, Mach 0.3), 16-ft Transonic Tunnel (1/30-scale model, Mach 0.4-1.25), the Unitary Plan Wind Tunnel (1/30-scale model, test sections 1 for Mach 1.6-2.5 and test section 2 for Mach 2.5-4.63), and the 20-Inch Mach 6 Tunnel (0.018-scale model, Mach 6). A Mach number range of 0.3 to 6.0 and an angle of attack range of -4 to +32 deg. were covered during these tests. In some cases multiple runs were made for a given Mach number and angle of attack range. All these results were processed, and mean lines were drawn through the data points for each

Mach No.	α range (deg.)	Gas Model	Flow Solver
1.25	-4, 2, 8, 16, & 24	P.G. Air	Transonic
1.60	2, 8, 16, & 24	P.G. Air	Transonic
1.60	-4, 2, 8, 16, & 24	P.G. Air	Hypersonic
2.50	-4, 0, 2, 8, 16, 24, & 32	P.G. Air	Hypersonic
4.00	-4, 2, 8, 16, 24, & 32	P.G. Air	Hypersonic
4.63	-4, 2, 8, 16, 24, & 32	P.G. Air	Hypersonic
6.00	-4, 2, 8, 16, 24, & 32	P.G. Air	Hypersonic

Table 1: Mach number and angle of attack range covered in the present study.

Mach number. This data was available for comparison with the computational results. In the comparison plots in this report, wind tunnel data are shown as lines and computed results as discrete points.

Mach 1.25 and 1.6

The results of computations for Mach 1.25 and 1.6 are listed in Tables 2 and 3, respectively. It may be noticed that for Mach 1.6 the computations were done using the transonic as well as the hypersonic flow solvers. As noted earlier, the FELISA software has two flow solvers—one applicable for transonic flows and the other applicable for hypersonic flows. It is expected that over the Mach number range 1.5–2.0 the two solvers would yield the same results. In order to confirm this, two sets of results were computed for Mach 1.6 —one using the transonic solver, and the other using the hypersonic solver. The wing upper surface C_p contours obtained from solutions using the transonic flow solver and the hypersonic flow solvers are shown in Fig. 6. It may be noticed from these plots that they are very similar. The computed aerodynamic data for these two cases are shown in Table 3. It may be noted that the two solvers yield results that are essentially the same. The maximum difference in the value of C_N is 0.0055, and the maximum difference in the values of C_m is 0.0017 both occurring at 24 deg. angle of attack.

Figure 7 shows a comparison of the computed C_N and wind tunnel data plotted versus angle of attack for Mach numbers 1.25 and 1.6. Computed values for Mach 1.6 include those obtained using the transonic flow solver as well as the hypersonic flow solver. The computed data points for transonic and hypersonic flow solvers lie on top of each other. Further, it may be observed from this figure that the computed C_N values compare well with the experimental data. Figure 8 shows a comparison of the computed C_m and wind tunnel data plotted versus angle of attack for Mach numbers 1.25 and 1.6. Here again the computed data points obtained using transonic and hypersonic flow solvers for Mach 1.6 lie on top of each other. However, the computed C_m values fall consistently below the experimental data and that the difference between the wind tunnel data and the computational result increase as the angle of attack is increased. As noted earlier, absence of boundary layer, particularly over the wing upper surface, would lead to differences in the shock locations at transonic and low supersonic speeds. This would results in differences between computed results and wind tunnel data.

Mach No.	α (deg.)	C_N	C_A	C_m	**Grid**	**Flow Solver**
1.25	-4	-0.1197	0.0842	-0.0924	Grid 1	Transonic
1.25	2	0.2144	0.0794	-0.1469	Grid 1	Transonic
1.25	8	0.5579	0.0696	-0.2075	Grid 1	Transonic
1.25	16	1.0054	0.0459	-0.2417	Grid 1	Transonic
1.25	24	1.4201	0.0283	-0.2156	Grid 1	Transonic

Table 2: Computed C_N, C_A, and C_m for X-34 for Mach 1.25

Mach No.	α (deg.)	C_N	C_A	C_m	**Grid**	**Flow Solver**
1.60	2	0.1228	0.0684	-0.0889	Grid 1	Transonic
1.60	8	0.4099	0.0591	-0.1325	Grid 1	Transonic
1.60	16	0.8123	0.0428	-0.1684	Grid 1	Transonic
1.60	24	1.2215	0.0331	-0.1699	Grid 1	Transonic
1.60	-4	-0.1575	0.0696	-0.0454	Grid 1	Hypersonic
1.60	2	0.1261	0.0648	-0.0885	Grid 1	Hypersonic
1.60	8	0.4152	0.0557	-0.1315	Grid 1	Hypersonic
1.60	16	0.8174	0.0398	-0.1670	Grid 1	Hypersonic
1.60	24	1.2270	0.0304	-0.1716	Grid 1	Hypersonic

Table 3: Computed C_N, C_A, and C_m for X-34 for Mach 1.6 using the transonic and hypersonic flow solvers.

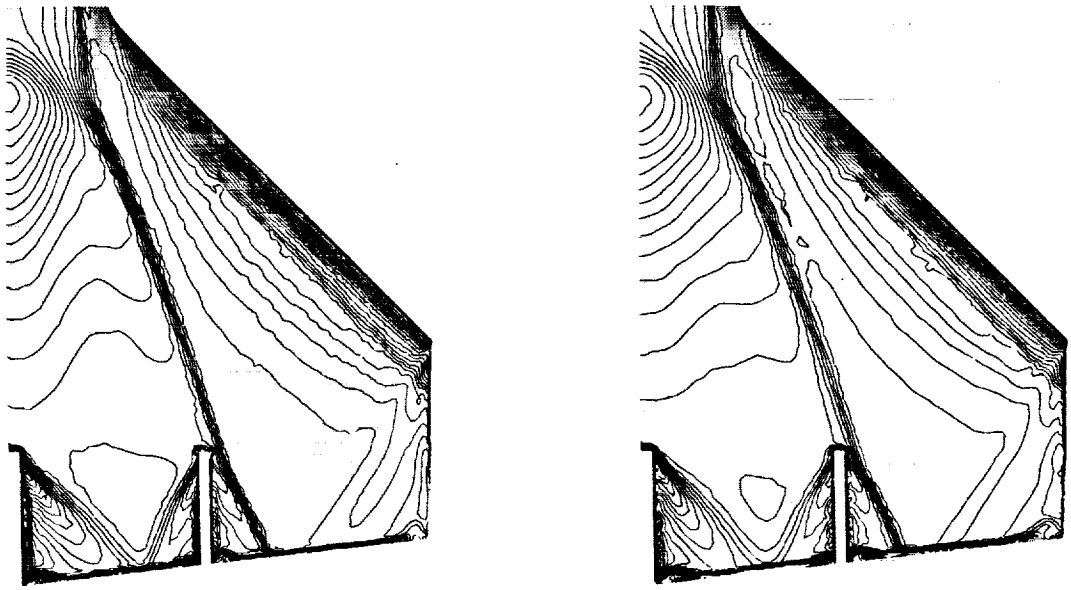

(a) Transonic flow solver

(b) Hypersonic flow solver

Figure 6: A comparison of wing upper surface C_p contour plots for Mach 1.6, α=16 deg.

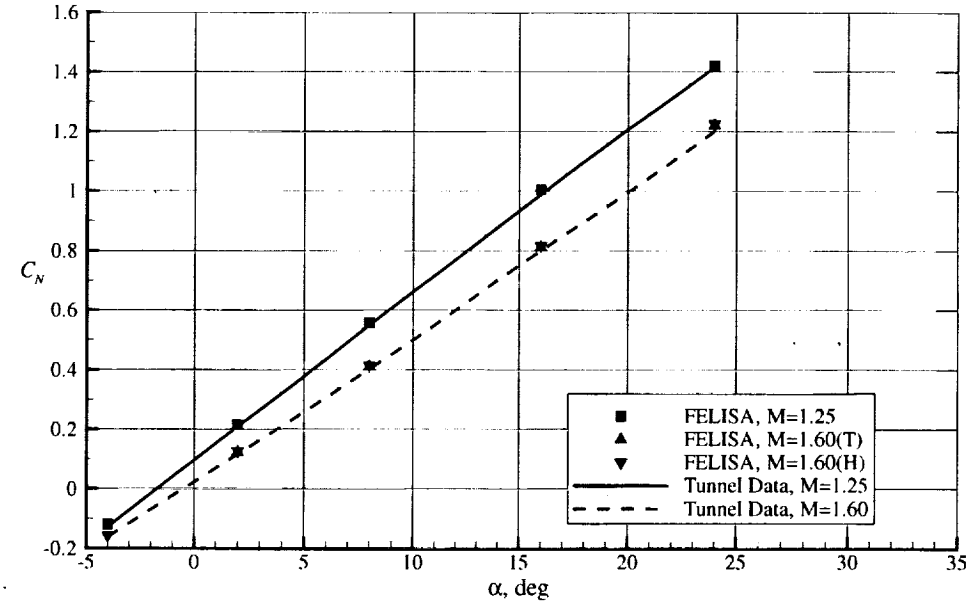

Figure 7: A comparison of computed and measured C_N for X-34 for Mach 1.25 and 1.6.

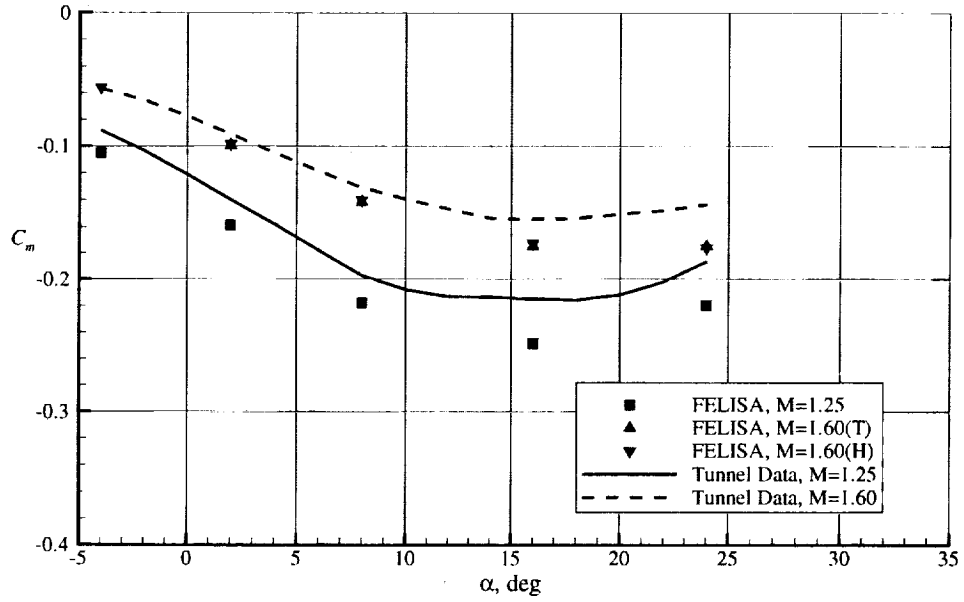

Figure 8: A comparison of computed and measured C_m for X-34 for Mach 1.25 and 1.6.

Mach No.	α (deg.)	C_N	C_A	C_m	Grid	Flow Solver
2.50	-4	-0.1449	0.0551	-0.0418	Grid 2	Hypersonic
2.50	2	0.0506	0.0489	-0.0465	Grid 2	Hypersonic
2.50	8	0.2569	0.0412	-0.0605	Grid 2	Hypersonic
2.50	16	0.5554	0.0324	-0.0734	Grid 2	Hypersonic
2.50	24	0.9055	0.0250	-0.0755	Grid 2	Hypersonic
2.50	32	1.2959	0.0178	-0.0798	Grid 2	Hypersonic
2.50	0	-0.0143	0.0514	-0.0437	Grid 3	Hypersonic
2.50	16	0.5562	0.0324	-0.0735	Grid 3	Hypersonic
2.50	24	0.9058	0.0249	-0.0753	Grid 3	Hypersonic
2.50	32	1.2964	0.0177	-0.0789	Grid 3	Hypersonic

Table 4: Computed C_N, C_A, and C_m for X-34 for Mach 4.0, 4.63, and 6.0

Mach 2.5

The computations for Mach 2.5 were done using two separate grids to determine the effect of grid refinement on the results. The first set of computations was done using a grid designated as grid 2. This grid has a grid spacing of 0.063 in. over the wing upper surface. The next set of computations was done using a grid designated grid 3. This grid has the spacing over the wing reduced to 0.033 in. The spacing in other regions of the grid were unaltered. The wing upper surface C_p contours obtained from solutions using grids 2 and 3 for $\alpha = 16$ deg. are shown in Fig. 9. It may be noticed from these plots that they are very similar. The aerodynamic coefficients obtained from solutions using grids 2 and 3 are shown in Table 4. An examination of this table reveals that the results obtained using the two grids are essentially the same. The maximum difference in the value of C_N is 0.0008 at 16 deg. angle of attack and the maximum difference in the values of C_m is 0.0009 at 32 deg. angle of attack.

The results of computations for Mach 2.5 listed in Table 4 are also shown plotted in Figures 10 and 11. It may be noted that for Mach 2.5, the computed C_N values for the two grids (grid 2 and grid 3) lie on top of each the other. The wind tunnel tests at Mach 2.5 were conducted in the NASA Langley Unitary Plan Wind Tunnel in two test sections, namely TS1 and TS2. Although the results from tests in TS2 are considered to be more reliable than those from tests in TS1, the C_N values from the two tests are plotted in Figure 10. It may be noted that the C_N values obtained in the two test sections are indistinguishable from each other. Further, the computed C_N values for Mach 2.5 compare well with the experimental data.

The computed C_m values are plotted in Figure 11 along with the experimental data. It may be noticed from this figure that the computed C_m values for the two grids lie on top of each other. This confirms that the initial grid (grid 2) was adequate for Mach 2.5 computations. The experimental data for the two test sections depart from each other beyond 10 deg. angle of attack. The computed values agree with the experimental data up to 10 deg. angle of attack; beyond this, the computed values fall below the experimental data. These differences are attributed to viscous effects.

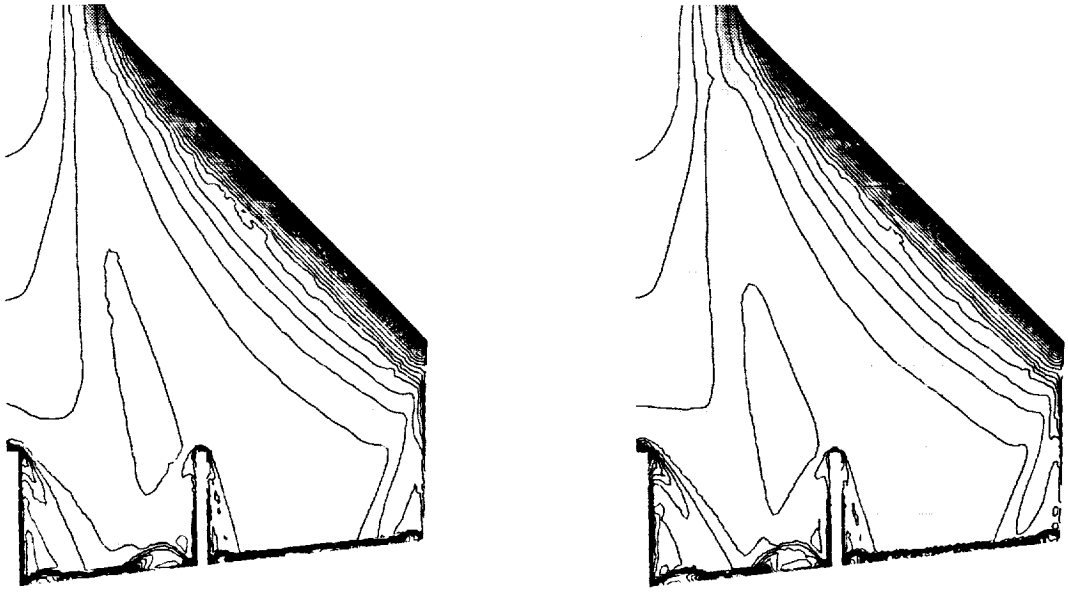

(a) Grid 2

(b) Grid 3

Figure 9: A comparison of C_p contour plots on the wing upper surface for Mach 2.5, α=16 deg.

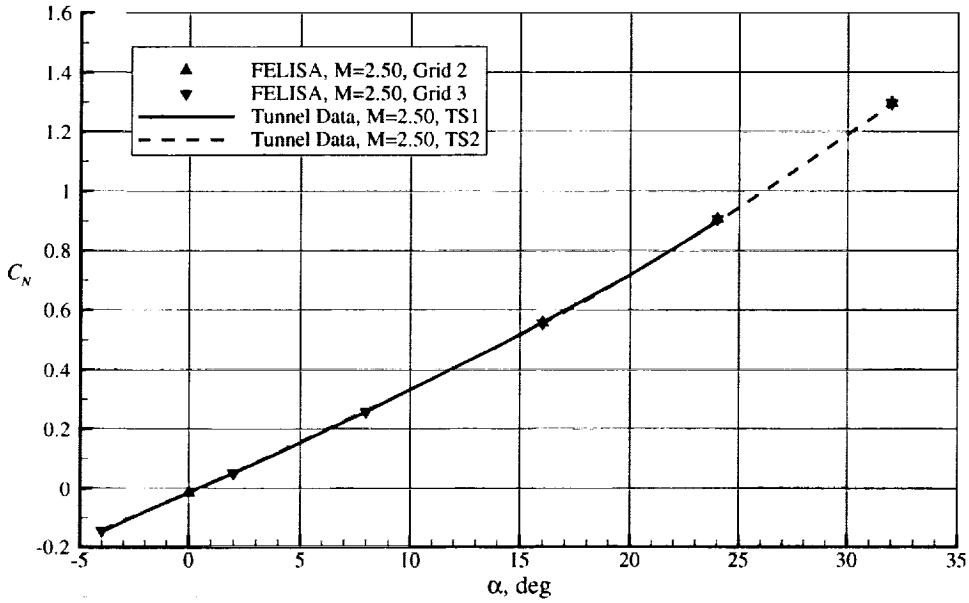

Figure 10: A comparison of computed and measured C_N for X-34 for Mach 2.5.

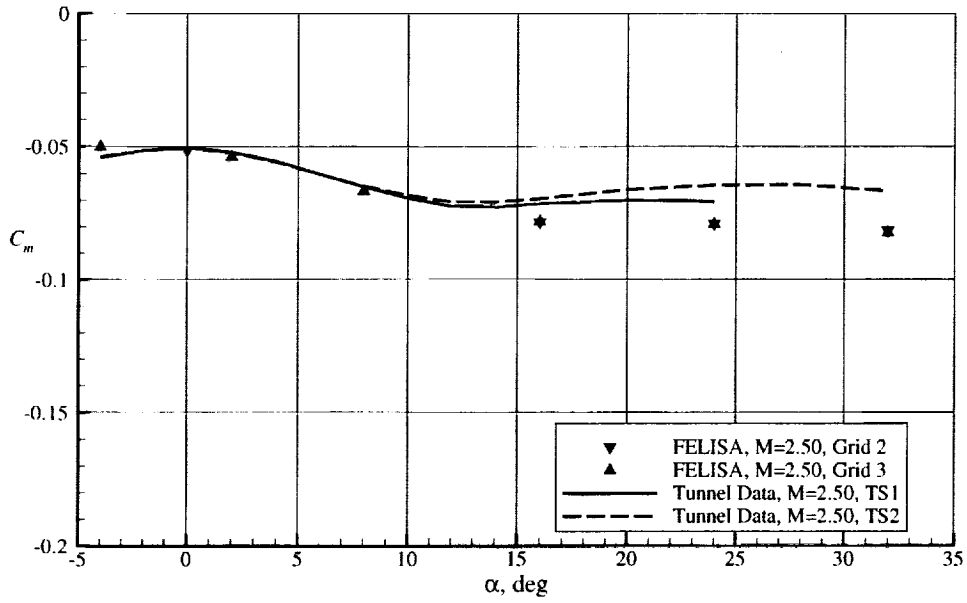

Figure 11: A comparison of computed and measured C_m for X-34 for Mach 2.5.

Mach No.	α (deg.)	C_N	C_A	C_m	Grid	Flow Solver
4.00	-4	-0.1239	0.0458	-0.0399	Grid 2	Hypersonic
4.00	2	0.0062	0.0389	-0.0305	Grid 2	Hypersonic
4.00	8	0.1499	0.0324	-0.0279	Grid 2	Hypersonic
4.00	16	0.4025	0.0243	-0.0286	Grid 2	Hypersonic
4.00	24	0.7241	0.0193	-0.0342	Grid 2	Hypersonic
4.00	32	1.1006	0.0144	-0.0435	Grid 2	Hypersonic
4.63	-4	-0.1181	0.0449	-0.0374	Grid 4	Hypersonic
4.63	-4	-0.1183	0.0448	-0.0371	Grid 2	Hypersonic
4.63	2	0.0036	0.0374	-0.0278	Grid 2	Hypersonic
4.63	8	0.1281	0.0305	-0.0230	Grid 2	Hypersonic
4.63	16	0.3706	0.0224	-0.0221	Grid 2	Hypersonic
4.63	24	0.6857	0.0175	-0.0273	Grid 2	Hypersonic
4.63	32	1.0626	0.0130	-0.0361	Grid 2	Hypersonic
6.00	-4	-0.1094	0.0444	-0.0322	Grid 2	Hypersonic
6.00	2	-0.0173	0.0358	-0.0243	Grid 2	Hypersonic
6.00	8	0.0989	0.0278	-0.0183	Grid 2	Hypersonic
6.00	16	0.3261	0.0194	-0.0143	Grid 2	Hypersonic
6.00	24	0.6369	0.0145	-0.0187	Grid 2	Hypersonic
6.00	32	1.0134	0.0113	-0.0262	Grid 2	Hypersonic

Table 5: Computed C_N, C_A, and C_m for X-34 for Mach 4.0, 4.63, and 6.0

Mach 4.0, 4.63, and 6.0

The results of computations for Mach 4.0, 4.63, and 6.0 are listed in Table 5, and are shown plotted in Figures 12 and 13. For these Mach numbers the computed C_N values compare well with the experimental data, except for Mach 4.0 at 24 and 32 degrees angles of attack, where the computed values are slightly smaller than the experimental data. It is suspected that these differences are effects of flow separation on the wing upper surface. The computed C_m values and the experimental data for Mach 4.0, 4.63, and 6.0 are shown plotted in Fig.13. The comparison in this case is much better than for Mach 1.25 and 1.6. For Mach 4.0 and 4.63 the agreement between the computed values and experimental values of C_m are good up to an angle of attack of 8 deg. Beyond this angle of attack the computed values are lower than the experimental values, and the differences increase as the angle of attack is increased. For Mach 6.0, there are small differences (0.0030 to 0.0035) up-to an angle of attack of 16 deg., with the computed values consistently below the measured values. Beyond this angle of attack, the differences increase. The differences in the C_m values at higher angles of attack are attributed to the effects of flow separation on the wing upper surface. Separation over the wing upper surface (near the trailing edge) results in positive pressures over parts of the elevons, and because of the distance between the elevons and the pitching moment reference point, leads to nose-up pitching moment.

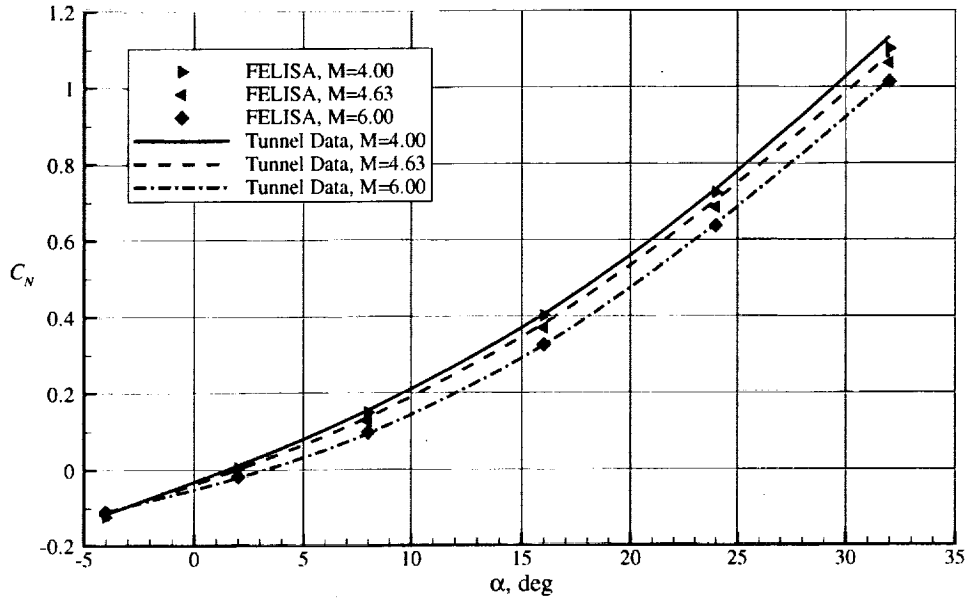

Figure 12: A comparison of computed and measured C_N for X-34 for Mach 4.0 to 6.0

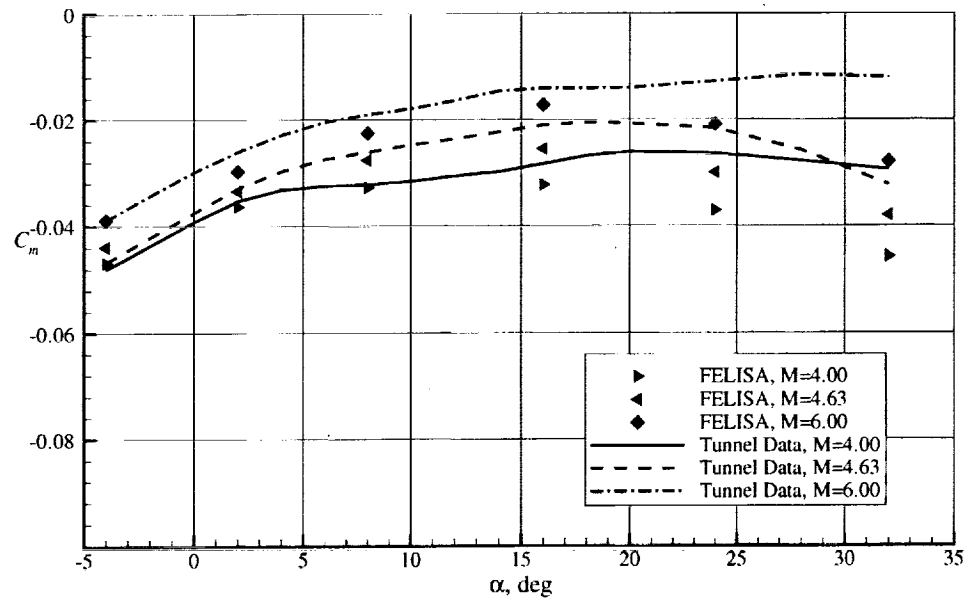

Figure 13: A comparison of computed and measured C_m for X-34 for Mach 4.0 to 6.0

Conclusions

The results of a computational study conducted on the Orbital Sciences X-34 vehicle to compute the inviscid longitudinal aerodynamic characteristics are presented. The computational results for a Mach number range of 1.25 to 6.0 are compared with available aerodynamic data from wind tunnel tests on the X-34 scale models. The comparison showed that inviscid FELISA software yields normal force coefficients that compare well with wind tunnel data over the entire Mach number and angle of attack ranges (-4–32 degrees). The computed pitching moment coefficients compared well at Mach numbers 2.5 and above, at angles of attack of up to 12 deg.; beyond this angle of attack, the agreement was not good. At these Mach numbers, the differences between the present (inviscid) computational results and the wind tunnel data are attributed to a large extent to the viscous effects which lead to flow separation, particularly over the wing upper surface at large angles of attack. At lower Mach numbers (1.25 and 1.6) there were significant differences between computed and measured pitching moment coefficient values. These differences are also attributed to viscous effects. At these Mach numbers, the absence of boundary layer on the wing upper surface leads to differences in the shock locations which in turn result in differences in the computed and measured aerodynamic data.

Acknowledgments

The author wishes to express his gratitude to Mr. K. J. Weilmuenster and Dr. K. Sutton of the Aerothermodynamics Branch (AB), NASA Langley Research Center for many helpful discussions during the course of this work. The author also wishes to thank Mr. G. J. Brauckmann of the AB for providing the experimental data used in this paper for comparison. The work described herein was performed at Lockheed Martin Engineering & Sciences Company in Hampton, Virginia, and was supported by the Aerothermodynamics Branch, NASA Langley under the contract NAS1-96014. The technical monitor was Mr. Weilmuenster.

References

[1] Freeman, Jr., D.C., Talay, T.A., and Austin, R.E., "Single-Stage-to-Orbit—Meeting the Challenge," Acta Astronautica, Vol. 38, Nos.4–8, pp. 323-331, 1996.

[2] Peiro, J., Peraire, J., and Morgan, K., "FELISA System Reference Manual and User's Guide," Tech. Report, University College of Swansea, Swansea, U.K., 1993.

[3] Frink, N.T., Pirzadeh, S., and Parikh, P., "An Unstructured-Grid Software System for Solving Complex Aerodynamic Problems," NASA CP-3291, pp. 289-308, May 9-11, 1995.

[4] Samereh, J., "GridTool: A Surface Modeling and Grid Generation Tool," NASA CP 3291, May 1995.

REPORT DOCUMENTATION PAGE

Form Approved
OMB No. 0704–0188

1. AGENCY USE ONLY *(Leave blank)*	2. REPORT DATE	3. REPORT TYPE AND DATES COVERED
	April 2001	Contractor Report

4. TITLE AND SUBTITLE
Inviscid Flow Computations of the Orbital Sciences X-34 Over a Mach Number Range of 1.25 to 6.0

5. FUNDING NUMBERS
C NAS1-96014
WU 242-80-01-01

6. AUTHOR(S)
Ramadas K. Prabhu

7. PERFORMING ORGANIZATION NAME(S) AND ADDRESS(ES)
Lockheed Martin Engineering & Sciences Company
C/O NASA Langley Research Center
Hampton, VA 23681–2199

8. PERFORMING ORGANIZATION REPORT NUMBER

9. SPONSORING/MONITORING AGENCY NAME(S) AND ADDRESS(ES)
NASA Langley Research Center
Hampton, VA 23681–2199

10. SPONSORING/MONITORING AGENCY REPORT NUMBER
NASA/CR–2001–210849

11. SUPPLEMENTARY NOTES
Langley Technical Monitor: K. James Weilmuenster

12a. DISTRIBUTION/AVAILABILITY STATEMENT
Unclassified-Unlimited
Subject Category 02
Distribution: Nonstandard
Availability: NASA CASI (301) 621–0390

12b. DISTRIBUTION CODE

13. ABSTRACT ***(Maximum 200 words)***

This report documents the results of an inviscid computational study conducted on the Orbital Sciences X-34 vehicle to compute its inviscid longitudinal aerodynamic characteristics over a Mach number range of 1.25 to 6.0. The unstructured grid software FELISA was used and the aerodynamic characteristics were computed at Mach numbers 1.25, 1.6, 2.5, 4.0, 4.63, and 6.0, and an angle of attack range of -4 to 32 degrees. These results were compared with available aerodynamic data from wind tunnel test on X-34 models. The comparison showed excellent agreement in C_N. The computed pitching moment compared well at Mach numbers 2.5 and higher, and at angles of attack of upto 12 deg. The agreement was not good at higher angles of attack possibly due to viscous effects. At lower Mach numbers there were significant differences between computed and measured C_m values. This could not be explained. Since the present computations are inviscid, the computed C_A was consistently lower than the measured values as expected.

14. SUBJECT TERMS	15. NUMBER OF PAGES
Unstructured Grid, Hypersonic Speed, CFD, Aerodynamic Loads	22
	16. PRICE CODE: A03

17. SECURITY CLASSIFICATION OF REPORT	18. SECURITY CLASSIFICATION OF THIS PAGE	19. SECURITY CLASSIFICATION OF ABSTRACT	20. LIMITATION OF ABSTRACT
Unclassified	Unclassified	Unclassified	UL